Occurrence of crop pests and diseases has largely increased in China since 1970

Wang, Chenzhi; Wang, Xuhui; Jin, Zhenong; Müller, Christoph; Pugh, Thomas A.M.; Chen, Anping; Wang, Tao; Huang, Ling; Zhang, Yuan; Li, Laurent X.Z.; Piao, Shilong

DOI:
10.1038/s43016-021-00428-0

Occurrence of crop pests and diseases has largely increased in China since 1970

Chenzhi Wang[1], Xuhui Wang[1*], Zhenong Jin[2], Christoph Müller[3], Thomas A. M. Pugh[4,5], Anping Chen[6], Tao Wang[7,8], Ling Huang[1], Yuan Zhang[1], Laurent Li[9], Shilong Piao[1,6,7]

Affiliations

1.Sino-French Institute for Earth System Science, College of Urban and Environmental Sciences, Peking University, Beijing 100871, China.

2. Department of Bioproducts and Biosystems Engineering, University of Minnesota-Twin Cities, St. Paul, Minnesota 55455, USA.

3.Climate Resilience, Potsdam Institute for Climate Impact Research, Member of the Leibniz Association, Potsdam 14473, Germany.

4.School of Geography, Earth and Environmental Sciences, University of Birmingham, Birmingham B15 2TT, UK.

5. Birmingham Institute of Forest Research, University of Birmingham, Birmingham B15 2TT, UK.

6. Department of Biology, Colorado State University, Fort Collins, CO 80523, USA.

7. Key Laboratory of Alpine Ecology, Institute of Tibetan Plateau Research, Chinese Academy of Sciences, Beijing 100101, China.

8. Center for Excellence in Tibetan Earth Science, Chinese Academy of Sciences, Beijing 100085, China.

9. Laboratoire de Meteorologie Dynamique, UPMC/CNRS, IPSL, Paris 75005, France.

*Correspondence to: xuhui.wang@pku.edu.cn

Abstract

Crop pests and diseases (CPD) are emerging threats to global food security, but trends in the occurrence of pests and diseases remain largely unknown due to the lack of observations for major crop producers. Here, based on a unique historical dataset with more than 5,500 statistical records, we found an increased occurrence of CPD in every province of China, with the national average rate of CPD occurrence increased by a factor of four (from 53% to 218%) during 1970-2016. Historical climate change is responsible for more than one-fifth of the observed increment of CPD occurrence (22% ±17%), ranging from 2% to 79% in different provinces. Among the climatic factors considered, warmer night-time temperature contributes most to the increasing occurrence of CPD (11% ± 9%). Projections of future CPD show that, at the end of this century, climate change will lead to increasing CPD occurrence to 243% ± 110% (SSP126) and 460% ± 213% (SSP585), whose magnitude largely depends on the impacts of warmer nighttime temperature and decreasing frost days. This observation-based evidence highlights the urgent need to accurately account for the increasing risk of CPD in mitigating the impacts of climate change on food production.

Main

Narrowing yield gaps is considered to be an effective strategy to feed the planet facing growing food demand and climate change[1, 2, 3]. While much attention has been paid to closing the yield gap through employing efficient irrigation[4] and improving nutrient managements[4, 5], the risk of crop pests and diseases (CPD), which may reduce the attainable yield by more than 50% [6, 7], has not been well assessed for major crop producers. Although the threat of CPD could be more severe under climate change[8,9], our understanding on CPD dynamics remains insufficient to address the challenge, partly because the occurrence of CPD, which largely determine the cost of CPD management [10, 11], is difficult to predict under diverse circumstances due to its complex interactions with climate and agronomic practices[12]. Understanding the change in CPD occurrence has become an urgency for sustaining food security[13].

Previous data-based assessments on CPD occurrence had to rely on controlled growth chambers or small-scale field experiments[14, 15] for single species of CPD. However, impact assessment for major food producers must consider the integrated impacts of different CPD species across broad production regions, ranging from ~10 Mha (like France) to more than 100 Mha (like China). This scale and extent cannot be well represented by few field/laboratory experiments. In addition, the magnitude of the dissemination and spread of CPD ranges from hundreds of kilometers to nearly tens of thousands of kilometers, e.g., the spread of the fall armyworm (*Spodoptera frugiperda*) across Africa and Asia from 2016 to 2019[16]. This scale of CPD dispersal cannot be studied with field/laboratory experiments alone. Models provide an alternative approach in understanding large-scale behaviors of CPD impacts[17]. Current models are more skillful in representing CPD damage through eco-physiological processes [18], but only have simplified representation of CPD occurrence, leaving it a critical knowledge gap[19]. The limitations of both experiments and models thus highlight the crucial need to study the CPD occurrence with observational data for major global crop producers [20, 21].

China is the world's largest producer of major cereals (rice, wheat and maize) feeding nearly 20% of the global population and has been increasingly suffering from CPD risks[22]. The occurrence area of CPD was assumed to have imposed a major threat to China's crop production[21]. For example, in 2019 the fall armyworm (*Spodoptera frugiperda*) alone spread over 26 provinces of China and infested more than 112 Mha of cropland[23], and is expected to cause larger damage in the coming years. Deustch et al. projected that both of rice and wheat production in China will suffer a lot from pests in the future[9], which highlights the need to better understand the changing CPD occurrence over China and its relationship with climate change. Here, we harmonized a unique dataset of long-term national statistical records about CPD occurrence in China. This dataset was based on more than 5000 surveying records of CPD occurrence since 1970 reported by the National Agricultural Technology Extension and Service Center (details see Methods). Applying this dataset, we further analyzed the impact of climate change on CPD occurrence over the past five decades in China.

CPD occurrence has increased fourfold since the 1970s

At the national scale, we found the average CPD occurrence area in China is 234 Mha (69 Mha - 378 Mha) during 1970-2016 (Supplementary Fig. 1). To minimize the effects of expanding crop planting area since 1970 over China[24] on investigating the change of CPD occurrence, in this study, we focused on the ratio of CPD occurring area to that of crop planting area (O_r) (see Methods section for further details). As Fig. 1 shows, O_r increased from 53%±33% in 1970 to 218%±103% in 2016, with an average increasing rate of 3.1% per year (Fig.1a). Spatially, O_r is higher in the North China Plains and the Middle-Lower Yangtze Plains, the two major crop production regions of China. Meanwhile, O_r is low in northern and southwest China. The trend of O_r is high (more than 4% yr^{-1}) in the northwestern and the southern regions but relatively slow (less than 2.5% yr^{-1}) in the northern and the southwestern regions.

The substantial increase in the CPD occurrence ratio is driven by a simultaneous increase in occurrence ratios of crop pests (O_r^P) and diseases (O_r^D) across different crops. Fig.2a,b compare the O_r^P and O_r^D between two periods (1970-1979 and 2010-2016) respectively. Specifically, the mean O_r^P of three stable crops of China (wheat, rice, maize) increased from 8.4%, 17.7%, 24.4% in the 1970s to 34.4%, 62.0%, 35.2% in the 2010s respectively. For diseases, the overall O_r^D was lower than that for pests, but there was also an evident increase of O_r^D for all crops from the1970s to the 2010s. The mean O_r^D of wheat, rice and maize increased from 2.2%, 9.8%, and 6.1% in the 1970s to 23.1%, 40.8%, and 20.1% in the 2010s, respectively.

Reflecting the increasing rates of both O_r^P and O_r^D of different crops, we find significant positive trends in O_r^P and O_r^D at the national scale (Fig. 2-c) with steeper slopes of O_r^P (1.34±0.17 % yr^{-1}, 0.75±0.06 % yr^{-1}) than of O_r^D (0.71±0.09 % yr^{-1},0.61±0.08% yr^{-1}) for both rice and wheat, while maize has steeper trends in O_r^D (0.29±0.08%yr^{-1} vs 0.50±0.2 %yr^{-1}). The Fig. 2d summarizes the major CPD occurrence over the past five decades, separated by CPD species groups and host crops at national scale. It is evident that the three stable crops (rice, wheat and maize) are the main hosts of CPD in China. Lepidoptera and Homoptera pests as well as fungus each account for substantial proportions of CPD occurrence.

Increasing CPD occurrence is partly attributed to changing climate

Next, we explored the relationship between O_r and potential driving factors. The occurrence of CPD is affected by numerous factors, including both climatic factors and cultural agronomic practices [6, 21]. Hence, we consider 12 factors including six climatic factors (daytime temperature (T_{max}), nighttime temperature (T_{min}), frost day frequency, precipitation, relative humidity and cloud cover condition), six management-related factors (fertilizer application rate, irrigation area, pesticide application rate, crop planting diversity, multiple cropping index, and GDP per capita) (See supplementary Table. 1 for details of these factors).

Fig. 3 shows correlations between detrend O_r and detrended potential driving factors. We found the correlations are statistically significant ($P<0.05$) for 9 of the 12 factors. The correlations between detrended anomalies of O_r and management related factors are generally weaker than that between detrended anomalies of O_r and climate variables, which also holds true if variables are not detrended (Supplementary table 2). The strongest correlations are found between detrended anomalies of O_r and nighttime temperature (T_{min}). The correlation coefficient between T_{min} and O_r is nearly 0.3 nationally ($R=0.29$, $P<0.01$) and positive for all provinces. The second strongest correlation was found between detrended anomalies of O_r and frost day frequency (FDF), which were consistently negative across all provinces but one (national coefficient is -0.23, $P<0.01$). Daytime temperature (T_{max}) is positively correlated with O_r nationally ($R=0.19$, $P<0.01$), but spatially divergent, with nearly 40% of provinces showing negative correlations (inset histogram of Fig. 3a). This spatial heterogeneous pattern highlights the need to further understand the relationship between O_r and T_{max}. Compared with temperature factors, the correlation coefficient of precipitation is smaller (national mean value is -0.13), which is also reflected by the large spatial variations in precipitation impacts[25].

Based on the correlation analysis, we found O_r significantly correlated with three temperature relevant factors (T_{min}, T_{max} and FDF) and precipitation. In order to test robustness of these relationships, we further calculated separate correlations between O_r^D, O_r^P and these four climate factors. As Supplementary Fig. 2a shows, the average of correlation coefficients between detrended occurrence ratios (O_r^D or O_r^P) and detrended nighttime temperature are all positive, while the mean values of the correlation coefficients with frost frequency are all negative. Cold nights and frost events are thus equally detrimental to both pests and disease, while frost events are only significantly correlated with wheat disease occurrence ratios, they are highly significantly correlated with pest occurrence ratios of all three crops considered here. Even though standard deviation of correlations of T_{max} is larger than that of T_{min}, the average correlation between daytime temperature and O_r^D and O_r^P are all positive.

This may also explain the lower correlation between T_{max} and O_r in Fig.2.

To account for spatial variations in quantifying the response of O_r to its climatic driving factors, we applied the Hierarchical Bayesian Model (see Methods), which allowed us to account for the spatial structure of CPD response to climatic factors, as well as its uncertainties, and proved to be effective in understanding the climate change impacts[26]. Moreover, the evident spatial heterogeneity of O_r and its correlation with climatic factors means that the statistical distribution of response of O_r to climate factors is not identical across provinces and Bayesian models do not require this. In this study, we applied the four climate factors and detrended O_r to build a statistical model that describes the heterogeneous response of O_r to changes in climatic factors. We found the responses of O_r to T_{min} and T_{max} are more sensitive than that to frost day and precipitation. The sensitivity of O_r to Tmin (S_{Tmin}) is positive in most provinces, the positive S_{Tmin} ranging between 0.08 %/^{o}C and 0.77 %/^{o}C. Results also show the magnitude of S_{Tmin} is larger in the North China Plain (NCP) and Huai river basin (Supplementary Fig. 3a) both of which are main crop producing regions in China. On the contrary, the sensitivity of O_r to T_{max} (S_{Tmax}) and to frost day frequency (S_{FDF}) exhibit a more heterogenous spatial pattern (Supplementary Fig. 3b, c). S_{Tmax}, ranging from -0.63 %/^{o}C to 0.55 %/^{o}C, is negative in northern and southern provinces but positive in central provinces, especially those provinces located in the Yangtze river basin (Supplementary Fig. 3b). The strong positive relationship between night-time temperature and O_r could result from the high proportion of nightly insects in categories of crop pests and disease in China [27] like lepidopterans, which accounts for 37% of the infected croplands (Fig. 2). The correlation analyses of O_r^P for different crops (Supplementary Fig.2-b) also supported this finding: The correlations between nighttime temperature and O_r^P of rice and maize pests are highly significant, and most of pests hosting these two crops belong to Lepidoptera (Fig.2-d).

Compared with the widespread negative impacts of warmer night-time temperature, the impacts of T_{max} on O_r are more complex and spatially divergent. We suggested that the variations of the optimal temperature of pests and diseases could explain the spatial heterogeneity. Crop pests and diseases threatening wheat and maize generally have lower optimal temperatures than those threatening paddy field crops

(Supplementary Fig. 4) and the negative correlation between wheat pest occurrence ratios and T_{max} in Supplementary Fig.2-b also supports this interpretation. The provinces having sizable percentage of paddy fields (Supplementary Fig. 5) tends to show positive S_{Tmax} (provinces along Yangtze river basin and a northeastern province, Heilongjiang). There are, however, exceptions in the southernmost provinces with sub-tropical climate (namely Guangdong, Guangxi Hainan and Yunnan; Supplementary Fig. 3b) show negative S_{Tmax}. This is probably due to higher growing season T_{max} over these provinces (Supplementary Table 3), which is close to or surpassed the optimal temperature of pests and diseases and increasing T_{max} thus may reduce pest occurrence.

We also tested the sensitivity of O_r^P and O_r^D across different crops to climate factors through Bayesian models. For wheat, the sensitivities of O_r^D and O_r^P to the four climate factors are similar, with mean values close to the 1:1 line and similar variance (Supplementary Fig.6-a). For both maize and rice, we observed the mean responses of O_r^P to nighttime temperature (S_{Tmin}^P) are stronger than that of O_r^D (Supplementary Fig.6-b,c). The strong responses of O_r^P for these two crops to nocturnal temperature are consistent with above correlation analysis on O_r. Lepidoptera pests have a distinct circadian rhythm and most of their activity is at night thus elevated nighttime temperatures may have a more pronounced effect than daytime temperatures on their physiological processes and behavior pattern.

Based on the above observation-derived relationship between climate factors and O_r, we estimated the contribution of climate change to the change of O_r since 1970 (Fig. 4). Overall, climate change contributes more than one fifth (mean value with one standard deviation: 22%±17%) to the change of O_r in China. This contribution shows large spatial heterogeneity ranging from 3% to 79% in different provinces (we excluded Shanghai, where crop land is very limited): it is generally higher in northern and southwest China (more than 20%) while lower in southeastern China (less than 20%) (Fig.4b). Among all climate variables considered, changes of temperature-related factors (T_{min}, T_{max}, FDF) account for more than 95% of the total climate change contribution (Fig.4a and Fig.4c). The positive contribution of warmer night-time temperature accounts the most (10.8%±9.7%), while day-time temperature has spatially heterogeneous contribution that account for 6.8%±6.1% of the total climate change contribution. The contribution of day and night temperature to the CPD occurring (Fig. 4a and fig. 4b) are strongest in the mid-latitude China (nearly north of 35°north latitude), which coincides with the top global wheat and maize producing region. This further highlights the alerting message from simple bioclimatic projection that the middle and high latitude regions are prone to intensification of CPD occurrence[28].

Climate-driven CPD occurrence change till the end of this century

Applying the same model to bias-corrected climate change projection under two different scenarios (SSP126 and SSP585, see Methods), we projected the climate-driven change of O_r from 2020 to 2100. The two scenarios considered represent the sustainable development pathway and high emission development pathway respectively, which means these two scenarios represent the 'best' and the 'worst' warming future. We found the O_r of China is projected to increase from 213% ±99% in 2020 to 243%±109% at the end of this century under the SSP 126 scenario and increase from 245%± 114% to 460%± 213% during the same period under the SSP 585 scenario (Fig. 5). Under the SSP 126 scenario, the increasing trend of projected O_r is relatively small (0.5%/year) and the O_r at the end of this century presents limited difference compared with the actual O_r in the 2016. On the contrary, O_r increases much faster under SSP 585 (2.9%/year) and at the end of century it will grow up to two-fold compared with current condition. Box plots in Fig. 5a represent projected changes of O_r under different time periods. The difference between the projected changes of O_r under SSP 585 and SSP 126 seems not evident at the near future (2020-2039) period while the gap between the box charts become wider since the mid-century (2040-2069) and the change of O_r under SSP 585 outclass that under SSP 126 at the end of this century obviously. This temporal distinction of the projected changes under these two scenarios reveals that, before the middle of this century, adopting the necessary strategy to alleviate the warming trend can favor reducing the risk of the rapid increase of CPD emergence of the end of this century.

We further explored the spatial pattern of the increase of O_r comparing the projected O_r (2054-2100) to the historical condition (1970-2016) (Fig. 5b and Fig. 5c). Spatial heterogeneity of change of O_r under these two scenarios is evident: under the SSP 126 scenario, the projected O_r increases more rapidly in the lower reaches of the Yangtze River and southwest China but under the SSP 585 scenario, the projected O_r shows a more obvious increase in northern and northwest China, especially provinces located in the Loess Plateau region, where agriculture is very sensitive to climate condition. Additionally, we found the spatial pattern of the increasing projected O_r under SSP 126 is similar to a continuation of the historical trends of O_r in many provinces. But even under SSP126, Fig 5 b show that projected O_r of southwestern provinces (Guangxi and Yunnan) are more intense than historical O_r implying that even in the 'best' future, the CPD occurrence of China could be worse regionally. As our Bayesian models are built on observed heterogeneous responses for O_r to climate drivers across the different provinces, projections take non-linear responses to changes in temperatures and precipitation into account. Still, the fact that CPD data is available only at a relatively high aggregation level in terms of spatial resolution and little distinction of specific pests and diseases, future works on more mechanical understanding of lifecycles, activities, and proliferation of multiple pest and diseases are desirable.

Admittedly, assessing crop yield reductions from the occurrence of CPD is not straightforward. A general framework to quantify crop yield loss risk has to combine CPD occurrence information with the crop damage intensity[29, 30]. A better understanding of the occurrence of CPD is thus the most direct warning signal to inform pest control strategies. Consequently, understanding the historical impacts of climate change on the CPD occurrence is fundamental for assessing the risk of crop yield reduction due to CPD in the warming future, providing additional perspective to previous studies on CPD effects through physiological activities, demography and dispersal for both crop pest[9, 31] and disease[32].

It should be noted that most previous studies often investigated the warming impacts using daily mean temperature as a proxy. This could be biased due to asymmetrical impacts of daytime versus night-time temperature on CPD occurrence that we find here, which responds stronger to nocturnal temperature. And this asymmetrical impact may amplify the extent of CPD occurrence in the high emission scenario, because of the faster warming trend of the nighttime temperature. We mapped the difference between the trend of nighttime temperature under these two scenarios (Supplementary Fig.7). The spatial heterogeneity of trend difference under the SSP 585 shows that the faster nighttime temperature warming is very distinct in the mid-and high latitude regions which can also explain the increase projected O_r in the northern China in Fig 5-b.

The impact of frost day on CPD occurrence is non-negligible. A direct evidence for this is all O_r^P across three main crops show significant negative correlations with frost days in China (Supplementary Fig.2-b). We also found the reduced frost day frequency may significantly contribute to the increasing O_r under the SSP 585 scenario, which is probably due to its strong association with the overwintering survival of many crop pests[9]. The higher overwintering survival means the larger population of the first generation of pest in the next year. Given the most of global breadbasket located in the temperate zones, the lowering frost day per year of this region in a warming future can exacerbate CPD occurrence in main crop producing regions, which may affect the global crop supply and international agricultural trade.

A considerable factor incurring uncertainties in our estimates is farmers' autonomous adaptations and agronomic practices, which may interact with climate change to affect CPD occurrence. For example, the practice of returning straw residues to the field is a policy promoted by the government to improved soil carbon content and fertility, but it can increase the risk of the CPD occurrence[33]. Additionally, modern agriculture is a combination of diversified agronomic practices so that its influence on CPD occurrence is difficult to evaluate. For example, agricultural intensification may favor increasing CPD occurrence but if the new anti-CPD cultivars are popularly used, this may decrease the risk of crop exposure to CPD[12]. Likewise, in our research, it could be observed that there is a leveling-off of O_r in recent years (Supplementary Fig. 8) and interestingly, the turning point of downturn in time-series O_r was just after a national crop protection policy implemented. This can also partly explain why climate change was found to be responsible for only one-fifth of the increasing trend of O_r.

Here, we compiled a long-term observational dataset on the occurrence of CPD and its climatic controls over China during the past five decades, filling a critical knowledge-gap[13]. Given the global reach of many of the pests considered, our results could have some representativeness over sub-tropical and temperate environments globally. The dataset consists of partially aggregated data in terms of geographic and species, so that the analysis is hampered by lack of details in some cases – such as in the question of which pests and diseases show which response across a temperature trajectory. Still, our findings highlight the major challenge posed by global warming, especially the rising nighttime temperature, for CPD occurrence. Assuming no fundamental changes in the diversity of pests and diseases under climate change, future climate warming could lead to more than 2-fold increment of CPD occurrence at the end of 21st century under the business-as-usual scenario, when asymmetrical impacts of warmer daytime and nighttime temperature, as well as the variability of frost day frequency, largely determine the magnitude of increment. Therefore, with the projected increasing risk of CPD occurrence, the next priority would be developing adaptive CPD management considering the integrated 'Crop-Environment-Pest and disease' system[34] in order to close the yield gap and feed the ever-rising population without damaging the environment and human health.

Methods

Datasets. We built the crop pests and disease (CPD) dataset of China based on the statistical records from the National Agricultural Technology Extension and Service Center, an institution directly subordinated to the Ministry of Agriculture and Rural Affairs of China. This institution manages and operates a bottom-up network that takes responsibility of crop protection and their specific work includes observing, surveying the CPD condition, guiding indigenous famers to control CPD and processing the statistics of crop protect condition.

This national network includes more than 2400 crop protection sites at the county level, more than 330 sites at the city level, which is an administrative unit between country and province in China, and 32 at the province level. The bottom-up workflow of CPD statistical records collecting is shown in Supplementary Fig.9. Each year, staffs of each county crop protection site observe the CPD condition regularly and when the CPD outbreaks they will survey the CPD emergence condition following the corresponding CPD surveying both of national standards and provincial standards because types of CPD may be different among different provinces sometime. Notably, only those CPD species that cause crop yield losses or failure will be surveyed of for staffs of crop protection sites. Thus, the most staff would follow the application manual of technical specifications for CPD surveying, which listed the major types of pests and diseases threating local crop yield based on historical records. At the end of each year, staffs serving at the county sites should collect the CPD surveying data of the whole county and process the statistics work and finally upload the results to the superior crop protection sites.

Thus, we used the statistical records at the province level, which can be considered reliable and homogenous, to reflect the emergence and impact of CPD at regional level. We collected more than 5500 records of CPD from 1970 to 2016 in China based on the long-time statistical data from the National Agricultural Technology Extension and Service Center. In this study, we used area of CPD occurrence

Agricultural data we used in this research includes yearly provincial crop planting area data (kilo ha), applying fertilizer quantity(ton), effective irrigation area (kilo ha), applying pesticide quantity(ton) and arable area (kilo ha) from 1970-2016, which we obtained from the National Bureau of Statistics of China. For socioeconomic data, we collected the per capita GDP from the same institution.

We also applied a crop distribution dataset to calculate weighted climate variables. The dataset used fine-resolution remote sensing imagery to obtain land-cover classifications and included the extent and location of cropland area in China[35].

Climate variables used in this study are based on the monthly CRUTS 4.01 climate data sets (http://doi.org/10/gcmcz3), covering the crop pest and disease time series period (1970-2016). The CRU TS 4.01 is a 0.5° x 0.5° resolution dataset of monthly climate variables derived from archives of more than 4000 climate station records[36]. Based on previous studies[31, 37, 38, 39], we selected 6 climate variables from the dataset that have potential impact on crop pest and disease: precipitation, minimum and maximum temperature, frost days frequency, vapor pressure and cloud cover percentage.

In this study, the climate factors we used to predict O_r are generated from Coupled Model Intercomparison Project Phase 6(CMIP 6) models in projections[40]. Compared with CMIP5, the future scenarios in CMIP6 have combined scenarios of the Shared Socioeconomic Pathways (SSPs)[41] and the Representative Concentration Pathways (RCPs)[42]. For example, SSP1-2.6 represents the future scenario incorporating SSP1-based socioeconomic development into the RCP 2.6-based energy-emissions-land use scenarios. Here, we used the daily output data including T_{max}, T_{min} and precipitation from 5 Earth system models (ESMs) under two scenarios SSP1-2.6(SSP126) and SSP5-8.5(SSP585) (Supplementary Table 4). These two scenarios represent low-emission scenario and high-emission scenario respectively. The dataset we used in the projecting O_r^{pd} was the latest version released by the Inter-Sectoral Impact Model Intercomparison Project Phase 3b. The bias of the dataset has been corrected and horizontal resolution has been statistically downscaled to 0.5-degree[43].

A limitation of data here is that the datasets we used for the analysis are not perfectly matched on the time scale. Previous researches proved that precipitation and humidity can affect the dissemination and infection of CPD. The sensitivity of CPD to these two factors may have an inner-annual variability because water demand is different during different growth stage of CPD for a specific specie and may be more different among different species[54] but the statistical records of provincial CPD condition are aggregated reports annually. Thus, we argued that the more detailed statistics with finer temporal resolution is more favorable to assess the influence of humidity and precipitation on the CPD.

Data processing. To ensure the spatial-temporal match of the CPD datasets with the climate records, we firstly removed provinces in which the time-series data cannot cover the period from 1970 to 2016. Additionally, considering the change of administrative regions of some provinces in China, we combined the provincial data to ensure the temporal uniformity. For example, Chongqing was not a provincial administrative region and belonged to Sichuan Province before 1997, thus we summed up the data of Chongqing and Sichuan of the period from 1998 to 2016 and treated them as one provincial region. Finally, we obtained data about the occurrence of CPD of 27 provincial regions (Supplementary Table 5).

We used the ratio of occurrence area of CPD (O_r) to offset the increasing crop planting area of China. The yearly O_r of each province is calculated as follows and its distribution is shown in Supplementary Fig. 10.

$$O_r = \frac{annual\ occurence\ area\ of\ CPD}{annual\ crop\ planting\ area} \qquad (1)$$

Notably, the O_r index is a comprehensive concept because it contains all crop pests and diseases emergence in whole year, which means it can exceed 100%. For example, consider a 100-ha wheat cropping field. In March, we find Specie A disease emergence in a 40-ha area of this field. In May, a 50-ha area suffers from Specie B disease and in September, Specie C pest invades a 30-ha area. In this scene, the O_r is 120%.

We converted the vapor pressure to the relative humidity based on the FAO methods[44]. To match with the yearly statistical record of CPD, we averaged the monthly climate variables and obtained the yearly data, including minimum temperature (T_{min}), maximum temperature (T_{max}), frost days frequency (Fdf), relative humidity (Rh), cloud cover percentage (Clc) and we summed up the monthly precipitation to get the annual amount of precipitation(P). We used the ratio of planting areas of each 0.5-degree grid as the weight then adjusted the climate variables to reflect the actual agricultural climate condition.

To prepare the climate future O_r, we also applied the same approach as we processed the historical climate factors to daily output data of 5 ESMs and obtained projected yearly climate factors (Supplementary Fig.11 and Supplementary Fig. 12). Notably, due to the lack of projected ground frost frequency, we converted the projected T_{min} to the projected Fdf with the same method as used in CRU TS 4.01 dataset[45].

Several studies pointed out that crop planting structure can enhance the robustness of agroecosystem and weaken the negative impact of disturbance on crop growth[46, 47, 48]. Thus, in this study, we also used the Shannon Diversity Index (SI) to quantify the crop diversity and the multiple crop index (MCI) to quantify the cropping system condition, which were viewed as potential factors influencing the CPD occurrence. The SI of each province can be calculated as follows:

$$\mathrm{SI} = -\sum_{i=1}^{3} P_i * (\ln P_i) \qquad (2)$$

$$P_i = \frac{S_{area}}{Crop_{area}} \qquad (3)$$

The MCI of each province can be calculated as follows:

$$\mathrm{MCI} = \frac{Crop\ plant\ area}{Arable\ area} \qquad (4)$$

The cropped area includes the three major crops (rice, wheat and maize) in China (Supplementary Fig.13 shows time series of three major crops production condition in China).

Analysis. Six climate variables (T_{max}, T_{min}, Fdf, Rh, P and Clc), five agricultural management variables (fertilizer quantity, irrigation area, pesticide quantity, crop diversity and MCI) and a socioeconomic factor, per capita GDP are regarded as the potential factors that can account for the occurrence of CPD (Supplementary Table.1). Firstly, we applied a correlation analysis to investigate whether there is a relationship between a potential factor and the O_r (Supplementary Table.2). To test the robustness of these correlations, we detrended variables if they have a significant trend from 1970 to 2016 or else we subtracted the mean value. Then we applied the correlation analysis in the anomaly of each factor and O_r. Fig. 3 shows the national correlation coefficient of different factors. Moreover, at provincial scale, we also analyzed the correlation between anomaly of factors and anomaly the O_r and plotted the histograms (Fig.2). The analyzed data met the assumptions of the statistical tests.

We further applied Bayesian hierarchical method to model the relationship between O_r and correlative variables. A hierarchical model is more flexible than a fixed model and its hierarchical structure can make the fitting more robust and easier to explain[26, 49, 50]. In this study, to avoid the illusory relationship caused by the trend of potential factors and the O_r, we also used the detrended factors and O_r to build the model. Correlation coefficient between O_r anomalies and these factors anomalies over

0.1 are deemed as they have correlated relationships. Thus we took T_{max},T_{min}, Fdf and P into this model based on the Fig.2. The relationship between O_r and the four potential climate factors which hold a robust correlation with O_r is modeled as follows:

$$(O_r)_{i,t} \sim Norm\left(\mu_{i,t}, \sigma_i^2\right) \quad (5)$$

$$\mu_{i,t} \sim Norm\left(\alpha 0_i + \alpha 1_i Tmax_{i,t} + \alpha 2_i Tmin_{i,t} + \alpha 3_i Fdf_{i,t} + \alpha 4_i P_{i,t},\ \sigma u_{i,t}^2\right) \quad (6)$$

In the formula, *i* represents the *i*-th province, *t* represents the *t*-th year. The tilde (~) indicates 'distributed as', T_{min} is the yearly minimum temperature, T_{max} is the yearly maximum temperature, Fdf represents the yearly frost day frequency and the P indicates the annual total precipitation. The prior distribution of σ_i^2 and $\sigma u_{i,t}^2$ follow an inverse Gamma distribution.

We assumed that the prior distribution of coefficients of covariables αk,k=0, … ,4 as normal distribution:

$$\alpha k \sim Norm(\beta_0, \sigma_{\alpha k}^2) \quad (7)$$

The β_0 is an initial constant (here we set it as zero) and we also assumed the hyper-prior distribution of $\sigma_{\alpha k}^2$ is inverse Gamma distribution.

The posterior distribution of each parameter was estimated by the MCMC (Markov Chain Monte Carlo) method and this process was conducted through Open BUGS[51, 52] and R (v 3.5.2). We run all models until convergence was reached, which was evaluated through both trace plot graphs and Gelman–Rubin convergence diagnostic values[53].With this method, we estimated all coefficients of covariables (αk,k=0, … ,4 and γk, k=0, … ,4) and Supplementary Fig.14- Fig.17 show the posterior distribution of $\alpha 1$-$\alpha 4$, which represent the sensitivity of O_r to corresponding factors.

The contribution of climate change to the change of O_r at province scale is calculated as follows:

$$\text{Climate contribution to } Or = \frac{Tr_c}{Tr_O} * 100\% \quad (8)$$

The Tr_c represents the sum of the trend of climate factors product by corresponding sensitivity coefficient and the Tr_O represent the actual trend of O_r.

Projection analysis in the future. Based on the historical climate-CPD relationship, we applied the projected climate factors to predict the yearly O_r of each province under the two scenarios at first. For each scenario, we obtained five sets of projected O_r from climate data output of 5 ESMs and we calculated their mean value and standard deviation. Then we calculated the change of national projected O_r to the national historical result at different time periods as equation 9 shows.

$$\text{The change of } O_r^{pd} = \frac{projected\ O_r - historical\ O_r}{historical\ O_r} * 100\% \quad (9)$$

The time slice of projected O_r includes near future (2020-2039), mid-century future (2040-2069) and end of century (2070-2100). At last, we compared the provincial change of mean projected O_r to the mean historical O_r. To ensure the comparability principle, we selected the period from 2054 to 2100.

Data availability

The CRUTS 4.01 climate data set is publicly available at https://catalogue.ceda.ac.uk/uuid/58a8802721c94c66ae45c3baa4d814d0 ; Two future scenarios datasets in CMIP6 is publicly available at https://www.isimip.org/gettingstarted/input-data-bias-correction/ ; Agricultural data at provincial scale is publicly open at https://data.stats.gov.cn/english/; The crop pests and diseases dataset is available at https://doi.org/10.6084/m9.figshare.16866736.v2

Code availability

All data were processed using MATLAB v2018b. Most of statistical analysis was carried out in MATLAB v2018b. The Bayesian hierarchical analysis was carried out in R studio (based on R v3.5.2) with the Open BUGS API. The figures were produced in Origin Pro 2020b and ArcGIS 10.7. Figure 2 was produced with MATLAB code (https://www.mathworks.com/matlabcentral/fileexchange/45639-hexscatter-m). Other codes are available upon request.

Acknowledgements

This study was supported by the National Natural Science Foundation of China (42171096). We thanked Mingzhu He, Qiang Liu and Lei Jin for their help in preparing the manuscript. We also thanked the reviewers for their constructive comments improving the manuscript from its earlier version.

Author Contributions Statement

X. W. designed the study. C. W. collected data and performed analyses. C. W., X. W., Z. J., C. M., S. P. wrote the manuscript. All authors contributed to interpretation of the results and manuscript revisions.

Competing interests

Authors declare no competing interests.

Figure Captions

Fig. 1 Spatial and temporal pattern of O_r. a. Time series of O_r from 1970 to 2016 and the distribution of the trend of each province: the dark blue line is the mean value of the time-series O_r at the country level and the blue fill area refers to the one standard deviation of time-series O_r. The histogram in the upper left is the distribution of provincial trend of O_r and the red dash line represents the mean trend b. Spatial pattern of the mean O_r from 1970 to 2016; c. Spatial pattern of the trend of O_r from 1970 to 2016.

Fig.2 National occurrence condition of different crop pests and diseases from 1970-2016. a. The comparison of pest occurrence ratios (O_r^P) between the 1970s and the 2010s across different hosts. The box chart reflects the distribution of O_r^P across different crops. Light green represents the O_r^P in the 1970s and the dark green represent values in the 2010s. b. The comparison of diseases occurrence ratios (O_r^D) between the 1970s and the 2010s.The box chart reflects the distribution of O_r^D across different crops. Light purple represents the O_r^D in the 1970s and dark purple represent that in the 2010s. c. Rising trend of O_r^P and O_r^D across different crops from 1970 to 2016. The column height represents the mean trend and the error bar represents one standard deviation. d. Sankey diagram summarizing major CPD occurring hosts and species from the 1970s to the 2010s at national scale. The percentages given in this figure represent the share of occurrence area of a specific type in total CPD occurrence area but the colors of different flows did not represent the degree of occurrence.

Fig. 3 Correlations between anomaly of factors and anomaly of O_r. In each subplot, the scatter represents the relationship between the anomaly of factor and the anomaly of O_r of all provinces and the correlation coefficient is labeled in the plot. The black line indicates the regression fitting results. The upper left histogram in subplot is the probability frequency distribution of the correlation coefficient of each province. A~I subplots represent the daytime temperature, nighttime temperature, frost day frequency, precipitation, relative humidity, cloud cover percentage, applying fertilizer quantity, irrigation area, applying pesticide quantity, crop diversity condition, multiple crop index and per capita GDP respectively.

Fig. 4 Contribution of climate change to change of O_r from 1970 to 2016. a. The contribution of different components to the change of O_r of each province. Upper panel shows the contribution of the four climate factors to the change of O_r of all provinces. Because several provinces in the upper panel is not clear enough to distinguish contribution of each climate factor, we marked them (provincial contributions of climate change to the corresponding change of O_r below 30%) with dash lines and mapped them in the lower panel. b. Spatial pattern of contribution of climatic change to the change of O_r from 1970 to 2016. The black labels represent the abbreviation of province names and supplementary table 5 shows the full names of all administrative units. c. Distribution of provincial absolute contribution of climate factors to the change of O_r. This half-violin figure shows the information of absolute contribution of four climate factors. The right part of the violin figure represents probability density distribution and the points with error bars represent the mean with one standard deviation. The left part of the violin figure applying the scatter to represent the specific distribution of the data.

Fig. 5 Change of O_r projection from 2020 to 2100 under two scenarios. a. The projected changes in O_r at different time periods. The box plots show the projected changes in O_r compared with historical result at different time periods. NF represents near future (2020-2039), MC represents mid-century (2040-2069), EC represents end of century (2070-2100). Red box and dark blue box also represent the projected changes under SSP 585 and SSP 126 respectively. b and c show spatial pattern of the increasing O_r between the historical result (mean O_r in 1970-2016) and projection (mean O_r in 2054-2100) under the SSP 126 and SSP 585 respectively.

References

1. Foley JA, *et al.* Solutions for a cultivated planet. *Nature* **478**, 337-342 (2011).
2. FAO. The future of food and agriculture—Alternative pathways to 2050.). Food and Agriculture Organization of the United Nations Rome (2018).
3. Tilman D, Balzer C, Hill J, Befort BL. Global food demand and the sustainable intensification of agriculture. *P Natl Acad Sci USA* **108**, 20260-20264 (2011).
4. Mueller ND, Gerber JS, Johnston M, Ray DK, Ramankutty N, Foley JA. Closing yield gaps through nutrient and water management. *Nature* **490**, 254-257 (2012).
5. Zhang W, *et al.* Closing yield gaps in China by empowering smallholder farmers. *Nature* **537**, 671-674 (2016).
6. Chakraborty S, Newton AC. Climate change, plant diseases and food security: an overview. *Plant Pathol* **60**, 2-14 (2011).
7. Oerke EC. Crop losses to pests. *The Journal of Agricultural Science* **144**, 31-43 (2005).
8. Bebber DP, Ramotowski MAT, Gurr SJ. Crop pests and pathogens move polewards in a warming world. *Nature Climate Change* **3**, 985-988 (2013).
9. Deutsch CA, *et al.* Increase in crop losses to insect pests in a warming climate. *Science* **361**, 916-919 (2018).
10. Delcour I, Spanoghe P, Uyttendaele M. Literature review: Impact of climate change on pesticide use. *Food Res Int* **68**, 7-15 (2015).
11. Ziska LH. Increasing Minimum Daily Temperatures Are Associated with Enhanced Pesticide Use in Cultivated Soybean along a Latitudinal Gradient in the Mid-Western United States. *Plos One* **9**, (2014).

12.Lamichhane JR, *et al.* Robust cropping systems to tackle pests under climate change. A review. *Agronomy for Sustainable Development* **35**, 443-459 (2014).

13.Bebber DP, Field E, Gui H, Mortimer P, Holmes T, Gurr SJ. Many unreported crop pests and pathogens are probably already present. *Global Change Biology* **25**, 2703-2713 (2019).

14.Bale JS, *et al.* Herbivory in global climate change research: direct effects of rising temperature on insect herbivores. *Global Change Biology* **8**, 1-16 (2002).

15.Garrett KA, Dendy SP, Frank EE, Rouse MN, Travers SE. Climate change effects on plant disease: Genomes to ecosystems. *Annu Rev Phytopathol* **44**, 489-509 (2006).

16.Hruska AJ. Fall armyworm (Spodoptera frugiperda) management by smallholders. *CAB Reviews* **14**, 1-11 (2019).

17.Sutherst RW, Constable F, Finlay KJ, Harrington R, Luck J, Zalucki MP. Adapting to crop pest and pathogen risks under a changing climate. *Wiley Interdisciplinary Reviews: Climate Change* **2**, 220-237 (2011).

18.Donatelli M, Magarey RD, Bregaglio S, Willocquet L, Whish JPM, Savary S. Modelling the impacts of pests and diseases on agricultural systems. *Agric Syst* **155**, 213-224 (2017).

19.Jones JW*, et al.* Toward a new generation of agricultural system data, models, and knowledge products: State of agricultural systems science. *Agric Syst* **155**, 269-288 (2017).

20.Miller SA, Beed FD, Harmon CL. Plant Disease Diagnostic Capabilities and Networks. 47, 15-38 (2009).

21.Bebber DP, Holmes T, Smith D, Gurr SJ. Economic and physical determinants of the global distributions of crop pests and pathogens. *New Phytol* **202**, 901-910 (2014).

22.Savary S, Willocquet L, Pethybridge SJ, Esker P, McRoberts N, Nelson A. The global burden of pathogens and pests on major food crops. *Nat Ecol Evol* **3**, 430-439 (2019).

23.https://www.natesc.org.cn/News/des?id=eaf064ae-6582-47c1-a9f3-a58969fd47b3&kind=HYTX (available at April 2021).

24.Piao S, *et al.* The impacts of climate change on water resources and agriculture in China. *Nature* **467**, 43-51 (2010).

25.Chown SL, Sorensen JG, Terblanche JS. Water loss in insects: an environmental change perspective. *J Insect Physiol* **57**, 1070-1084 (2011).

26.Bjorkman AD, *et al.* Plant functional trait change across a warming tundra biome. *Nature* **562**, 57-62 (2018).

27. National Agricultural Technology Extension and Service Center. *Technical specification manual of major crop pest and disease observation and forecast in China*. China Agriculture Press (2010).
28.Olfert O, Weiss RM, Elliott RH. Bioclimatic approach to assessing the potential impact of climate change on wheat midge (Diptera: Cecidomyiidae) in North America. *The Canadian Entomologist* **148**, 52-67 (2015).
29.Savary S, Teng PS, Willocquet L, Nutter FW. Quantification and modeling of crop losses: A review of purposes. *Annu Rev Phytopathol* **44**, 89-112 (2006).
30.Chakraborty S. Migrate or evolve: options for plant pathogens under climate change. *Glob Chang Biol* **19**, 1985-2000 (2013).
31.Deutsch CA, *et al.* Impacts of climate warming on terrestrial ectotherms across latitude. *P Natl Acad Sci USA* **105**, 6668-6672 (2008).
32.Chaloner TM, Gurr SJ, Bebber DP. Plant pathogen infection risk tracks global crop yields under climate change. *Nature Climate Change* **11**, 710-715 (2021).
33.Carvalho JLN, *et al.* Agronomic and environmental implications of sugarcane straw removal: a major review. *GCB Bioenergy* **9**, 1181-1195 (2017).
34.Savary S, Horgan F, Willocquet L, Heong KL. A review of principles for sustainable pest management in rice. *Crop Protection* **32**, 54-63 (2012).
35.Frolking S, *et al.* Combining remote sensing and ground census data to develop new maps of the distribution of rice agriculture in China. *Global Biogeochemical Cycles* **16**, 38-31-38-10 (2002).
36.Harris I, Jones PD, Osborn TJ, Lister DH. Updated high-resolution grids of monthly climatic observations - the CRU TS3.10 Dataset. *International Journal of Climatology* **34**, 623-642 (2014).
37.Biota M. Climate Warming and Disease Risks for Terrestrial. *Science* **1063699**, 296 (2002).
38.Scherm H. Climate change: can we predict the impacts on plant pathology and pest management? *Can J Plant Pathol* **26**, 267-273 (2004).
39.Cheke RA, Tratalos JA. Migration, patchiness, and population processes illustrated by two migrant pests. *Bioscience* **57**, 145-154 (2007).
40.Eyring V, *et al.* Overview of the Coupled Model Intercomparison Project Phase 6 (CMIP6) experimental design and organization. *Geoscientific Model Development* **9**, 1937-1958 (2016).
41.O'Neill BC, *et al.* The Scenario Model Intercomparison Project (ScenarioMIP) for CMIP6. *Geoscientific Model Development* **9**, 3461-3482 (2016).
42.van Vuuren DP, *et al.* The representative concentration pathways: an overview. *Climatic Change*

109, 5-31 (2011).

43.Lange S. Trend-preserving bias adjustment and statistical downscaling with ISIMIP3BASD (v1.0). *Geoscientific Model Development* **12**, 3055-3070 (2019).

44.Allen RG, Pereira LS, Raes D, Smith M. Crop evapotranspiration-Guidelines for computing crop water requirements-FAO Irrigation and drainage paper 56. *Fao, Rome* **300**, D05109 (1998).

45.Harris I, Osborn TJ, Jones P, Lister D. Version 4 of the CRU TS monthly high-resolution gridded multivariate climate dataset. *Sci Data* **7**,109 (2020).

46.Kahiluoto H, *et al.* Decline in climate resilience of European wheat. *P Natl Acad Sci USA* **116**, 123-128 (2019).

47.Folke C, *et al.* Regime Shifts, Resilience, and Biodiversity in Ecosystem Management. *Annual Review of Ecology, Evolution, and Systematics* **35**, 557-581 (2004).

48.Renard D, Tilman D. National food production stabilized by crop diversity. *Nature* **571**, 257-260 (2019).

49.Clark JS. Why environmental scientists are becoming Bayesians. *Ecology Letters* **8**, 2-14 (2005).

50.Clark JS, Gelfand AE. A future for models and data in environmental science. *Trends in Ecology & Evolution* **21**, 375-380 (2006).

51.Gelfand AE, Smith AFM. Sampling-Based Approaches to Calculating Marginal Densities. *J Am Stat Assoc* **85**, 398-409 (1990).

52.Lunn D, Spiegelhalter D, Thomas A, Best N. The BUGS project: Evolution, critique and future directions. *Stat Med* **28**, 3049-3067 (2009).

53.Brooks SP, Gelman A. General methods for monitoring convergence of iterative simulations. *J Comput Graph Stat* **7**, 434-455 (1998).

54.Gregory PJ, Johnson SN, Newton AC, Ingram JS. Integrating pests and pathogens into the climate change/food security debate. *Journal of Experimental Botany* **60**, 2827-2838 (2009).

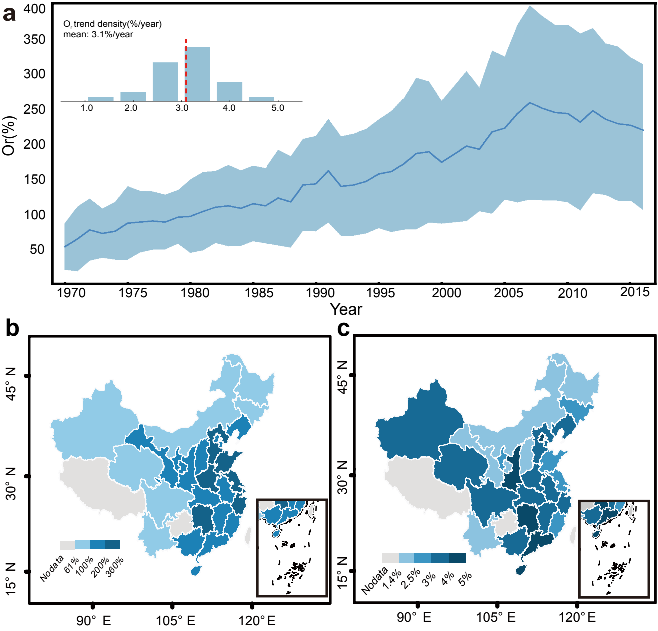
a
Or trend density(%/year)
mean: 3.1%/year
1.0
2.0
3.0
4.0
5.0
Or(%)
Year
b
Nodata
61%
100%
200%
360%
45° N
30° N
15° N
90° E
105° E
120° E
c
Nodata
1.4%
2.5%
3%
4%
5%
45° N
30° N
15° N
90° E
105° E
120° E

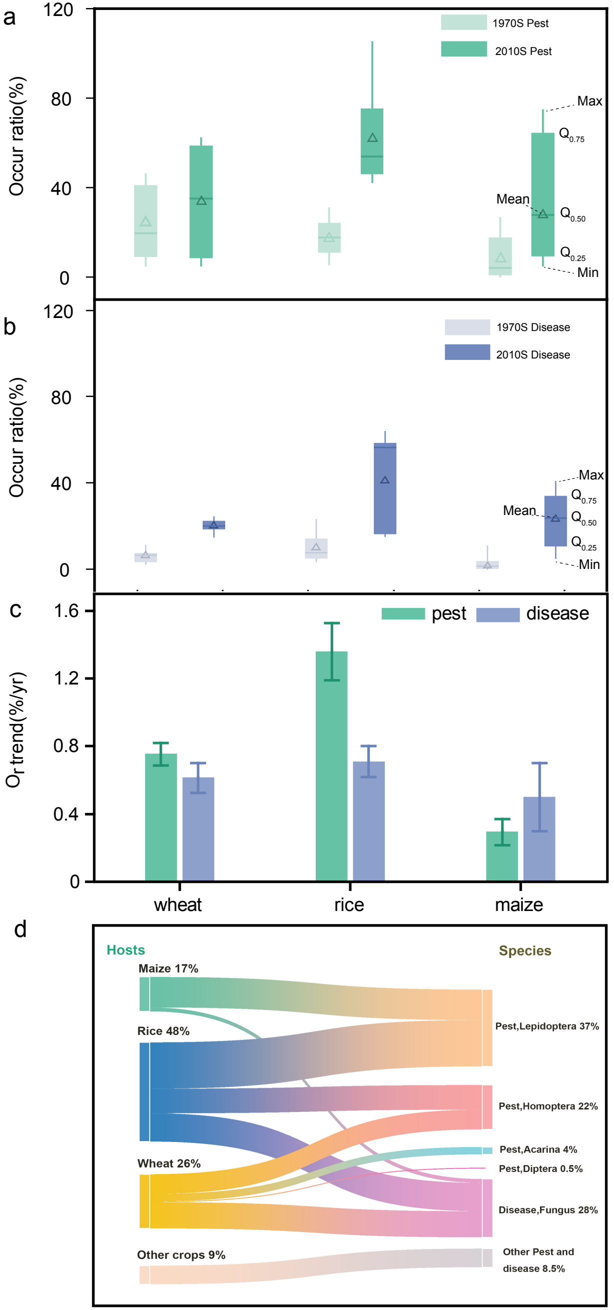
a
Occur ratio(%)
120
80
40
0
1970S Pest
2010S Pest
Max
$Q_{0.75}$
Mean
$Q_{0.50}$
$Q_{0.25}$
Min
b
Occur ratio(%)
120
80
40
0
1970S Disease
2010S Disease
Max
$Q_{0.75}$
Mean
$Q_{0.50}$
$Q_{0.25}$
Min
c
O_r trend(%/yr)
1.6
1.2
0.8
0.4
0
pest
disease
wheat
rice
maize
d
Hosts
Species
Maize 17%
Rice 48%
Wheat 26%
Other crops 9%
Pest,Lepidoptera 37%
Pest,Homoptera 22%
Pest,Acarina 4%
Pest,Diptera 0.5%
Disease,Fungus 28%
Other Pest and
disease 8.5%

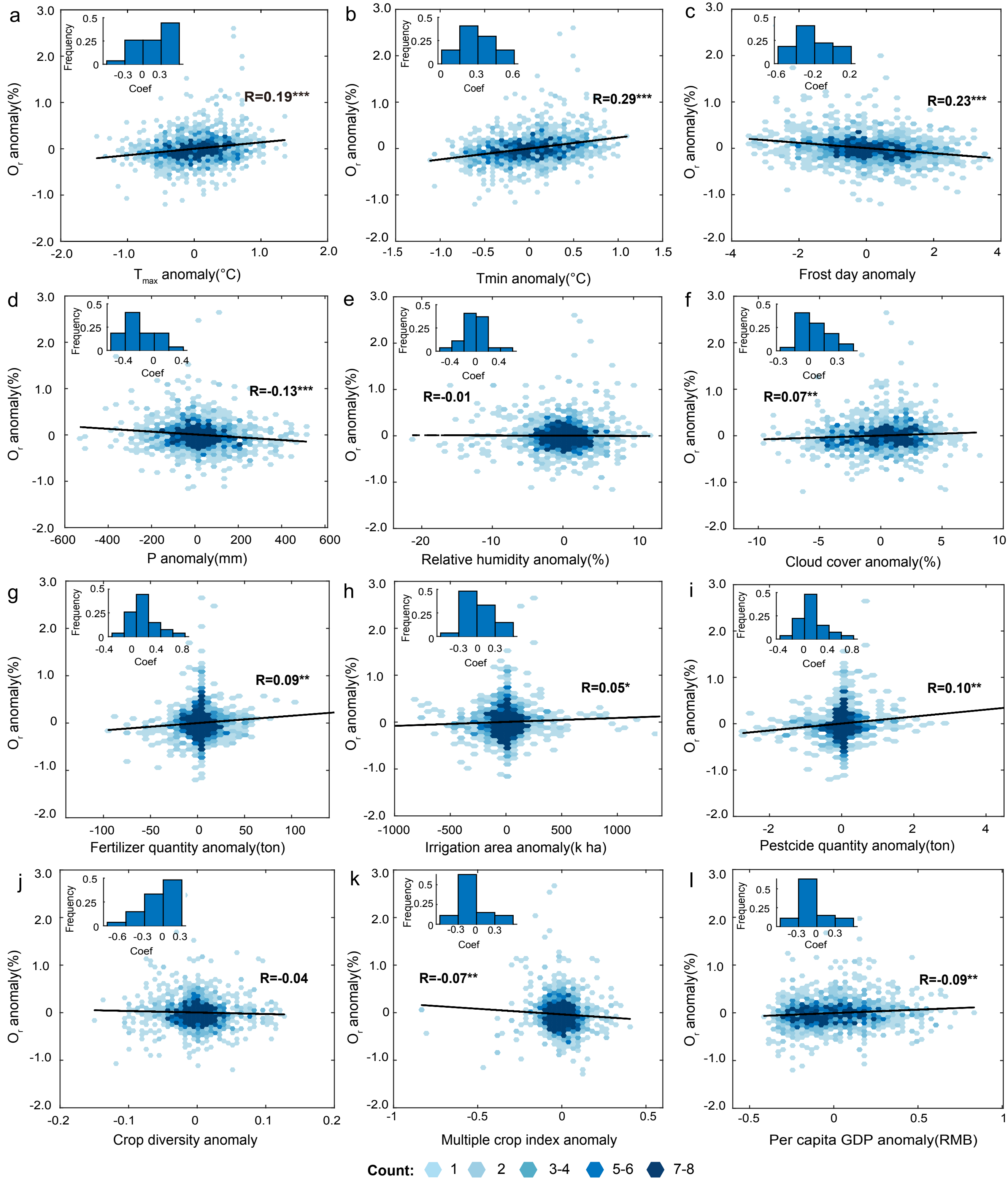
a
R=0.19***
T_{max} anomaly(°C)
b
R=0.29***
Tmin anomaly(°C)
c
R=0.23***
Frost day anomaly
d
R=-0.13***
P anomaly(mm)
e
R=-0.01
Relative humidity anomaly(%)
f
R=0.07**
Cloud cover anomaly(%)
g
R=0.09**
Fertilizer quantity anomaly(ton)
h
R=0.05*
Irrigation area anomaly(k ha)
i
R=0.10**
Pestcide quantity anomaly(ton)
j
R=-0.04
Crop diversity anomaly
k
R=-0.07**
Multiple crop index anomaly
l
R=-0.09**
Per capita GDP anomaly(RMB)
O_r anomaly(%)
Frequency
Coef
Count: 1 2 3-4 5-6 7-8

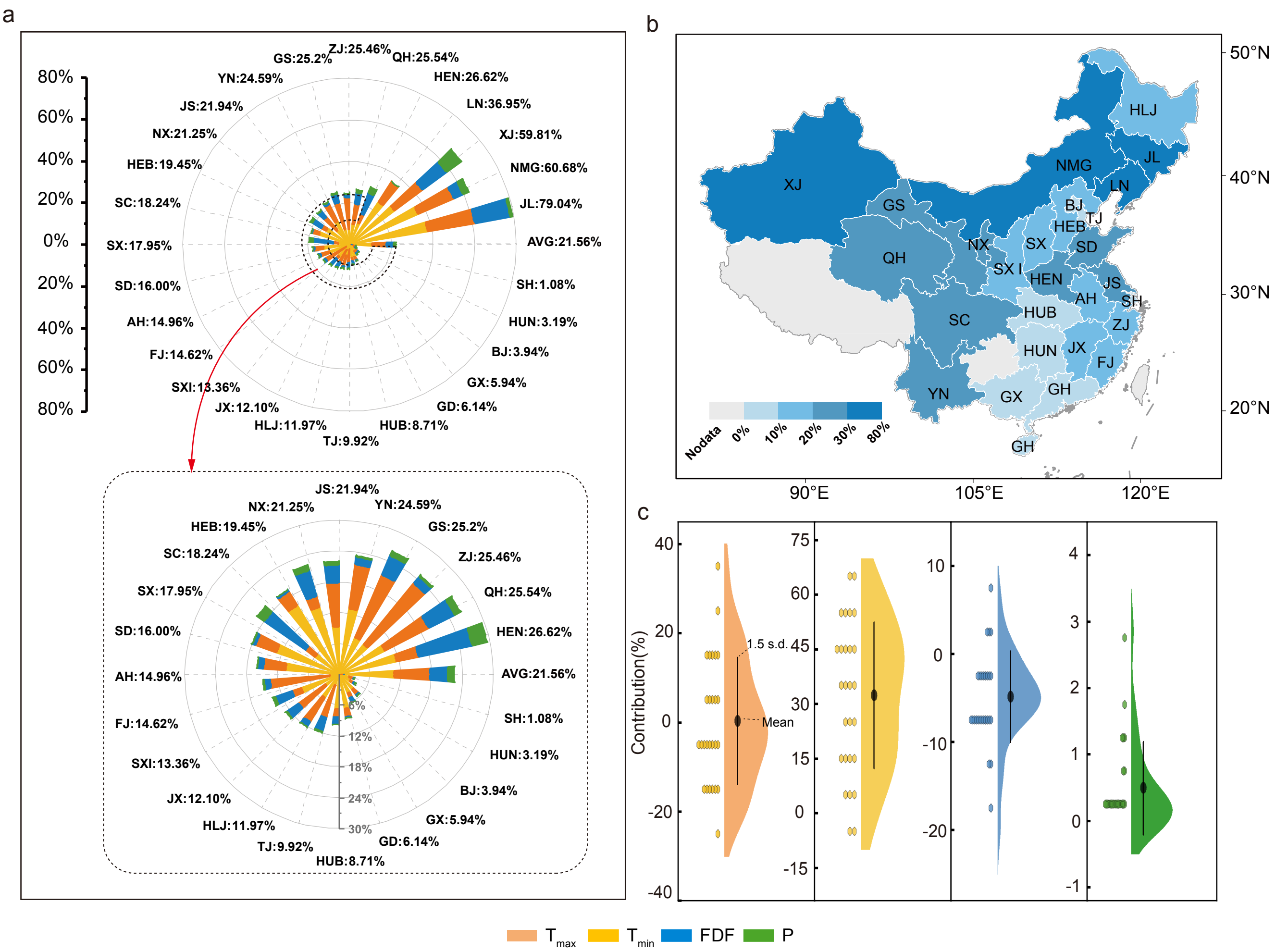

a
80%
60%
40%
20%
0%
20%
40%
60%
80%
GS:25.2%
ZJ:25.46%
QH:25.54%
HEN:26.62%
YN:24.59%
LN:36.95%
JS:21.94%
XJ:59.81%
NX:21.25%
NMG:60.68%
HEB:19.45%
JL:79.04%
SC:18.24%
AVG:21.56%
SX:17.95%
SH:1.08%
SD:16.00%
HUN:3.19%
AH:14.96%
BJ:3.94%
FJ:14.62%
GX:5.94%
SXI:13.36%
GD:6.14%
JX:12.10%
HUB:8.71%
HLJ:11.97%
TJ:9.92%
6%
12%
18%
24%
30%
b
XJ
GS
QH
NX
SX I
SC
YN
NMG
HLJ
JL
LN
BJ
TJ
HEB
SX
SD
HEN
AH
JS
SH
HUB
ZJ
HUN
JX
FJ
GX
GH
Nodata
0%
10%
20%
30%
80%
50°N
40°N
30°N
20°N
90°E
105°E
120°E
c
Contribution(%)
1.5 s.d.
Mean
T_{max}
T_{min}
FDF
P

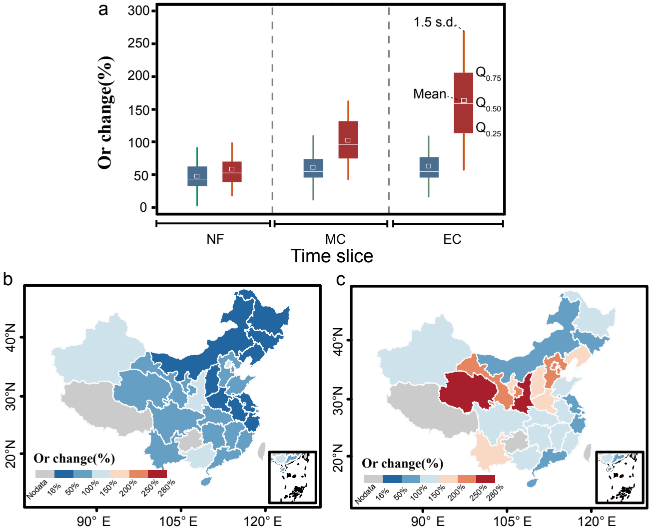

a
Or change(%)
300
250
200
150
100
50
0
1.5 s.d.
$Q_{0.75}$
Mean
$Q_{0.50}$
$Q_{0.25}$
NF
MC
EC
Time slice
b
c
40°N
30°N
20°N
Or change(%)
Nodata
16%
50%
100%
150%
200%
250%
280%
90° E
105° E
120° E